

Manifestation of function-follow-form in cultured neuronal networks

Vladislav Volman¹, Itay Baruchi¹ and Eshel Ben-Jacob^{1,2}

¹ School of Physics and Astronomy, Raymond & Beverly Sackler Faculty of Exact Sciences, Tel-Aviv University, Tel-Aviv 69978, Israel

² The Center for Theoretical Biological Physics, University of California at San Diego, La Jolla, CA 92093-0319, USA

E-mail: eshel@tamar.tau.ac.il

Received 17 December 2004

Accepted for publication 11 May 2005

Published 31 May 2005

Online at stacks.iop.org/PhysBio/2/98

Abstract

We expose hidden function-follow-form schemata in the recorded activity of cultured neuronal networks by comparing the activity with simulation results of a new modeling approach. Cultured networks grown from an arbitrary mixture of neuron and glia cells in the absence of external stimulations and chemical cues spontaneously form networks of different sizes (from 50 to several millions of neurons) that exhibit non-arbitrary complex spatio-temporal patterns of activity. The latter is marked by formation of a sequence of synchronized bursting events (SBEs)—short time windows (≈ 200 ms) of rapid neuron firing, separated by longer time intervals (seconds) of sporadic neuron firing. The new dynamical synapse and soma (DSS) model, used here, has been successful in generating sequences of SBEs with the same statistical scaling properties (over six time decades) as those of the small networks. Large networks generate statistically distinct sub-groups of SBEs, each with its own characteristic pattern of neuronal firing ('fingerprint'). This special function (activity) motif has been proposed to emanate from a structural (form) motif—self-organization of the large networks into a fabric of overlapping sub-networks of about 1 mm in size. Here we test this function-follow-form idea by investigating the influence of the connectivity architecture of a model network (form) on the structure of its spontaneous activity (function). We show that a repertoire of possible activity states similar to the observed ones can be generated by networks with proper underlying architecture. For example, networks composed of two overlapping sub-networks exhibit distinct types of SBEs, each with its own characteristic pattern of neuron activity that starts at a specific sub-network. We further show that it is possible to regulate the temporal appearance of the different sub-groups of SBEs by an additional non-synaptic current fed into the soma of the modeled neurons. The ability to regulate the relative temporal ordering of different SBEs might endow the networks with higher plasticity and complexity. These findings call for additional mechanisms yet to be discovered. Recent experimental observations indicate that glia cells coupled to neuronal soma might generate such non-synaptic regulating currents.

1. Introduction

It is now widely accepted that the brain informatics capabilities rely on neuro-plasticity combined with function-follow-form schemata, yet to be discovered. Much effort has been devoted to understanding how temporal pattern of activities at different locations in the brain is related to their physical (anatomical)

linkages [1–3]. The goal is to reveal the possible function-follow-form schemata by performing reverse engineering between the observed activity of the network (function), and the structural physiological properties of the network (form).

Considering the complexity of the brains' hierarchical organization, complementary and comparative studies of systems on all levels are required. Indeed, studies of

function-follow-form range from cultured networks through *in vitro* slices, to the level of the cortex [4–8]. Comparisons between these systems deserve special care, keeping in mind the profound differences between them. In particular, proper analysis methods for placing the recorded activity of these different networks within common presentation schemata must be used [8–10] if conclusions drawn from the study of one system are to be applied to the others.

1.1. The advantage of cultured networks

Here, we present new findings about the function-follow-form schemata, deduced from the analysis of cultured networks' activity of different forms, and make comparison to generic model simulations. The cultured networks provide relatively simple and well-controlled model systems for investigations of long-term (weeks) individual neuron activity at different locations by using a multi-electrode array [11, 12]. By analogy with the connectivity network's representation of the multi-channel recorded brain activity, the cultured network's activity can also be represented in terms of connectivity networks (function). In this case, the individual neuron locations are linked according to the correlation in their activities.

Utilizing lithographic methods, it is possible to engineer networks of different forms. In particular, engineered networks of sizes ranging from 10^{-2} mm² (small) through 1 mm² (medium) to 10² mm² (large), with a corresponding specified number of neurons ranging from 10² through 10⁴ to 10⁶, have been intensively studied [11, 13, 14].

Another major advantage of cultured networks is that their activity can be directly and even quantitatively (for the smaller ones) compared with model simulations [15, 16]. Here, we utilize the dynamical soma and synapses (DSS) model in which the neuron's soma is described by the Morris–Lecar dynamics, and the neurons are connected via dynamical synapses, as described by Tsodyks *et al* [17] (appendix B).

1.2. Questions posed by the spontaneous activity

The cultured networks spontaneously form from a dissociated mixture of cortical neurons and glia cells drawn from 1-day-old Charles River rats. The cells are spread homogeneously over a lithographically specified area of Poly-D-Lysine for attachment to the recording electrodes. Subsequently, the neurons send dendrites and axons to form a wired network. Although this process is self-executed with no externally provided guiding stimulation or chemical cues, a relatively intense dynamical activity is spontaneously generated within several days. As we show in the next section, the spontaneous activity is marked by the formation of synchronized bursting events (SBEs)—short time windows during which most of the recorded neurons participate in relatively rapid firing. These SBEs are separated by long (seconds to minutes) intervals of sporadic neuronal firing. It has been shown that the statistical properties of the SBEs time series and the individual neuron's activity can be captured by model simulations [15, 16]. The results of the model's performance are described in the next section.

In section 3 we describe the additional organizational motifs observed in the activity of large cultured networks. It

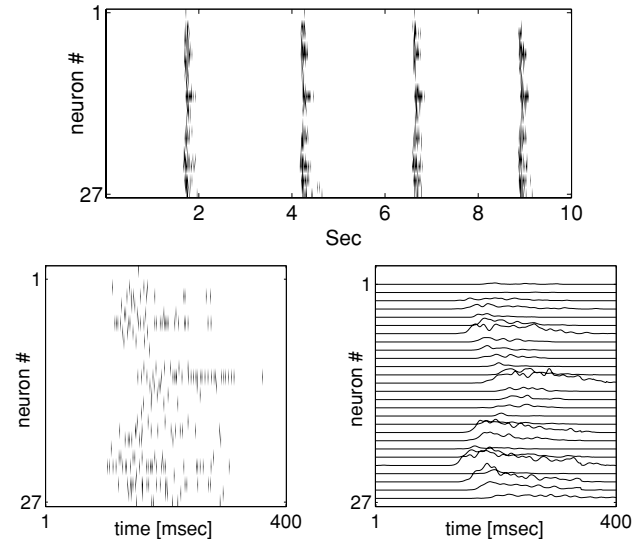


Figure 1. Top: formation of SBEs in the recorded activity of cultured networks. The time axis is divided into 10^{-2} s bins. Each row is a binary bar-code representation of the activity of an individual neuron, i.e. the bars mark detection of spikes. Note that each neuron has its own pattern of activity within a given SBE, and each SBE has its own internal pattern of neuronal activity. Bottom left: zoomed view of the synchronized bursting event. During the SBE, each neuron has its specific spiking profile. Bottom right: the average density representation of a SBE.

has been found that [8, 13], for some large networks, the SBEs might be classified as belonging to several distinct groups with each group representing a synchronized bursting event with a well-defined spatio-temporal internal structure. In contrast, the activity of small and medium-sized neuronal networks does not exhibit any such organizational motifs. This observation supports the notion of unitary, or elementary, networks about 1 mm³ in size, based on the following reasoning. The elementary time scale of neuronal activity is 10^{-3} s, while the propagation speed of action potentials along the axon is 1 m s⁻¹, yielding a characteristic length scale of 1 mm. In the cortex, 1 mm³ of tissue contains about 10^5 neurons, which corresponds to a cultured network of 1 mm² and 10^4 neurons. Hence, we define a unitary (or elementary) network as having $O(10^4)$ neurons in an area of 1 mm², i.e. corresponding to the medium-sized cultured networks. Higher density cultures grown in an area of 1 mm² form a web of neuronal clusters linked by axon bundles [7]. This is a hint that the cells 'are programmed' to form networks with special characteristics. By the same token, when 10^6 neurons are spread over 10² mm², they are free to form a homogeneous fabric of 10^2 coupled elementary networks. The measurements presented here were performed from electrode arrays of 10² mm². It has been proposed that the existence of sub-groups of SBEs in these large networks reflects the co-existence of functionally distinguishable coupled elementary networks [8].

The above features may be captured with the extended version of our model neuronal network, which takes into account the non-uniform distribution of synaptic connectivity.

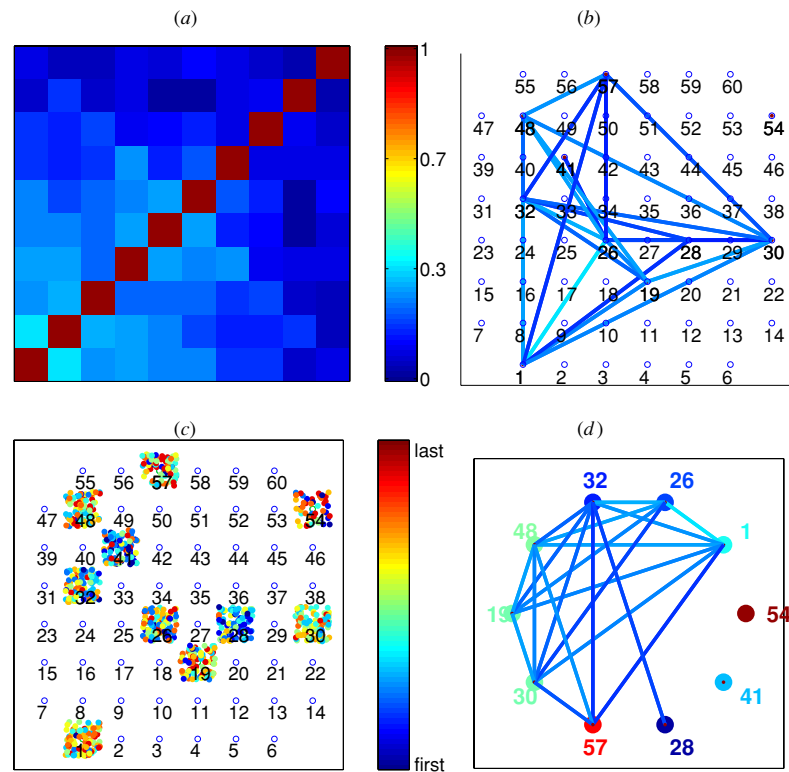


Figure 2. The internal dynamics of neurons during the SBE, for a typical medium-sized cultured network. The analysis has been performed on the data recorded from ten active electrodes. (a) The neuron correlation matrix, shown to demonstrate the statistical dependences between the activities of different neurons in the network during the bursting event. The color code of the correlation matrix is shown on its right. (b) The projection of the neuron correlation matrix onto the physical space of network’s electrodes gives information about the dependence of correlations on the physical location of neurons. To provide a better understanding about this relation, pairs of active electrodes are linked by the lines colored according to the level of correlation between the corresponding neurons (the color code is the same as that for the neuron correlation matrix). (c) The pattern of activity propagation through a network reveals that, during the bursting event, most of the neurons are activated almost simultaneously. The activity propagates from the early activated neurons (blue) to the late ones (red). (d) The correlation circle (constructed as explained in the text) is shown to demonstrate the interplay between network’s functional organization (correlations) and causal relations between different neurons in the network. For a typical medium-sized network, most of the neurons in the network are activated almost simultaneously, and the level of correlations between the neurons is nearly the same.

The results of this extended model are shown in section 4, where we also compare the performance of the model with that of cultured networks. Finally, in section 5 we discuss the possible regulatory mechanisms underlying the dynamics of cultured networks. We propose that these schemata can be attributed to the combined action of underlying glia fabrics.

2. Observations and modeling of unitary neuronal networks

The spontaneous activity of cultured networks is marked by the formation of synchronized bursting events—short (~ 200 ms) time windows during which most of the recorded neurons participate in relatively rapid firing. A typical raster plot visualization of such activity is presented in figure 1. The SBEs are separated by long intervals of sporadic neuronal firing. We describe each SBE as a matrix of N (number of neurons) vectors, each representing the temporal pattern of activity, or firing rate of a specific neuron (a row in the raster plot). As can be seen from figure 1, each SBE has its

own internal pattern of neuronal firing. Both the firing rate and the time-series statistical properties can greatly vary from neuron to neuron. While some neurons fire only 1–2 spikes per SBE, others can fire as many as 20 spikes per SBE. The individual neuron activity also varies from one SBE to another. To take into account these variations in the firing rate, one can define the average density of neuronal firing during the SBE by averaging the activity over many synchronized bursting events. An example of such average density representation is shown in figure 1. It is also seen that the average density reflects fairly well the general structure of the SBE.

The relations between different neurons during the bursting event are further revealed by calculating the neuron correlation matrices (see appendix A for technical details). The resulting matrix, shown in figure 2(a), indicates that for medium-sized (unitary) cultured networks, most of the neurons have similar, albeit relatively low level of correlation in their activities. To obtain information about the dependence of correlations on the spatial locations of neurons, we project the matrix of neuron correlations onto the physical space of network’s electrodes, and link neuron pairs by lines colored

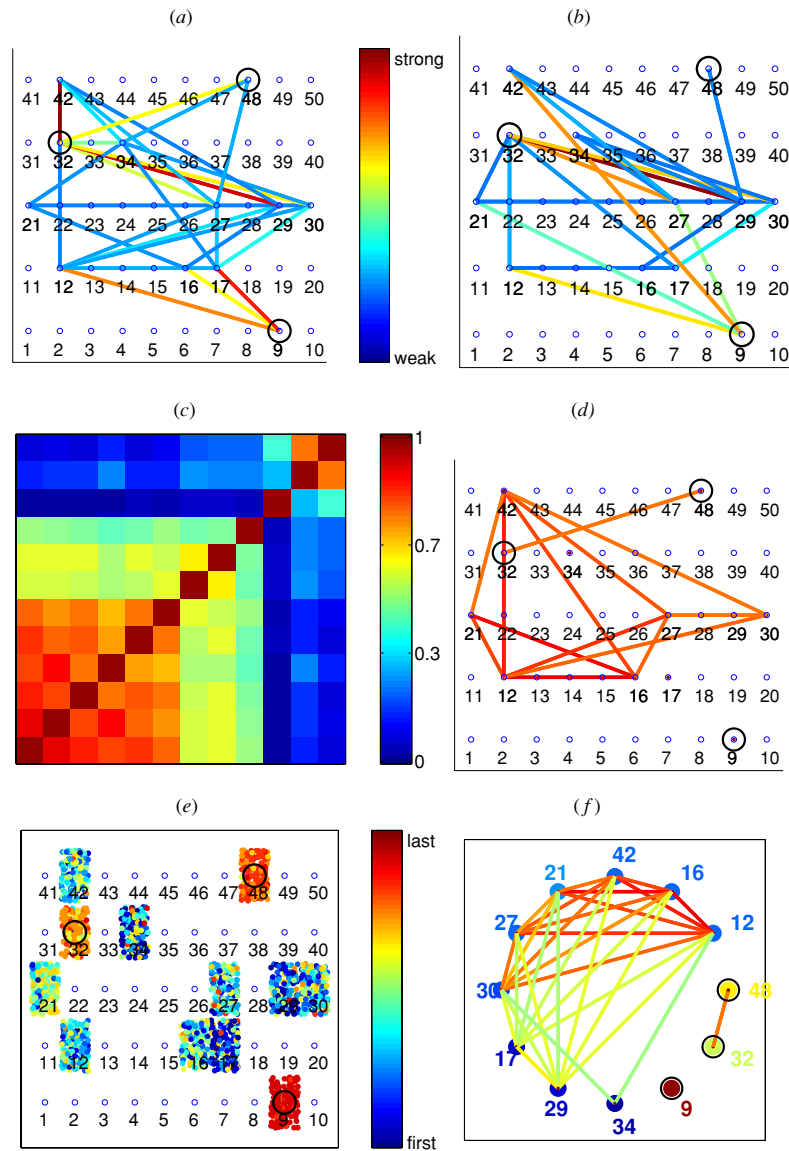


Figure 3. The internal dynamics of neurons during the SBE, for a simulated network with all-to-all synaptic connectivity. For better comparison with the experimental observations (see figure 2), we show the results for twelve neurons randomly sampled from a model network. Because pairs of neurons in the model network are reciprocally connected, we show the maps of synaptic connectivity for the cases of (a) A_{ij} matrix and (b) A_{ji} matrix. (c) The neuron correlation matrix for the model unitary network. Note that the structure of the matrix is block-like, with larger block corresponding to the excitatory model neurons, and smaller (upper) block to the inhibitory ones. (d) The projection of the neuron correlation matrix onto the space of model network's 'electrodes', obtained for the activity of model unitary network. (e) The map of activity propagation through the model network is shown to demonstrate uniform activation of the neurons. Note that the model inhibitory neurons (marked with circles) are activated at the end of the SBE. (f) The correlation circle for a model network with uniform connectivity has a structure similar to that of a unitary network, with uniform coloring of vertices and uniform level of correlations (compare with figure 2).

according to the level of correlation (figure 2(b)). The resulting projection indicates that the activity of a medium network is not spatially restricted; rather, the active electrodes are spread uniformly over the recording area. Next, to gain insight into the causal motifs associated with the activity of the network, we plot, for each SBE, the relative temporal ordering of neuronal activation during the burst. We use color code to distinguish between neurons activated early in the bursting event (blue) from those activated at the end of it (red). The timing of

neuronal activation may vary from burst to burst, as shown in figure 2(c). Each dot in the cluster of color dots around an electrode is the activation timing of the neuron (whose activity is recorded by that electrode), at a specific SBE. The resulting pattern of activity propagation shown in figure 2(c) suggests that, for the unitary network, most of the neurons in the network are activated almost at the same time.

Further, we wish to determine the relation between the pattern of correlations and the characteristic pattern of activity

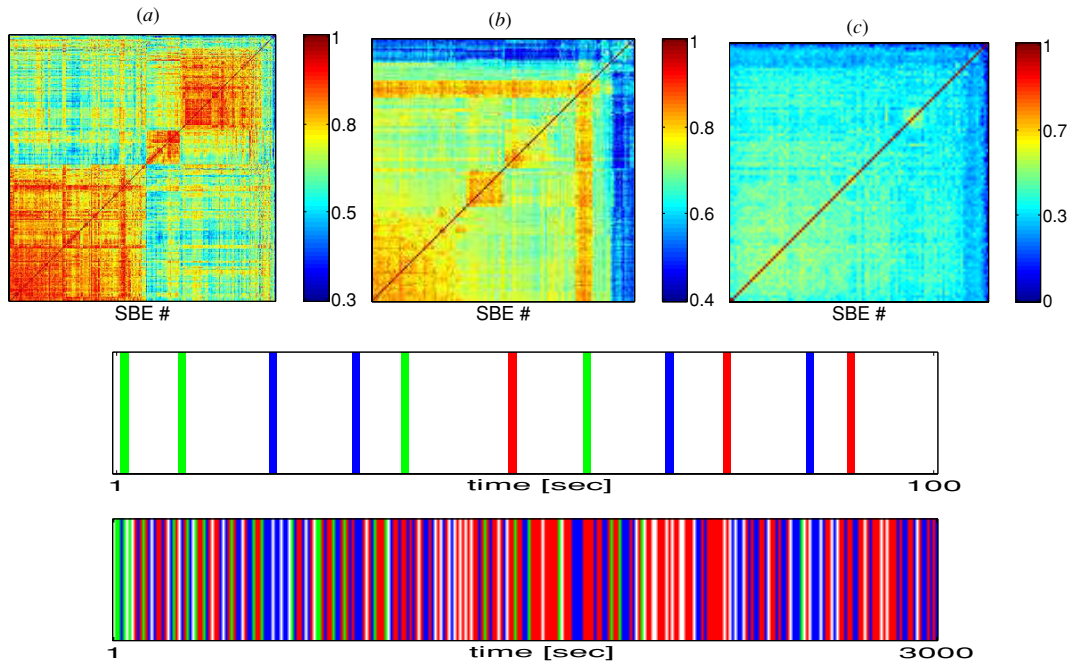


Figure 4. Top: the SBE correlation matrices for recordings from three different cultured networks. Each element (n, m) in the matrix represents the level of $EC_{n,m}$ by a color code. (a) An example of the SBE correlation matrix obtained for large network ($O(10^6)$ neurons), showing that there exist three distinct groups of SBEs. (b) Yet another example of the SBE matrix, exhibiting a band of highly correlated SBEs. (c) For comparison, the SBE correlation matrix for the medium-sized cultured network is shown, to stress that the appearance of blocks depends on the size of a network. Middle: the temporal sequence of SBEs for the activity of a typical large cultured network which exhibits three kinds of bursting events. The SBEs of different kinds have been assigned different colors, as explained in the text. Bottom: a zoomed out view of SBE sequence is shown to demonstrate the existence of unique temporal ordering in the appearance of different bursting events. Shown in the figure is the SBE series, constructed for the activity of a network with its corresponding SBE matrix shown in (a).

propagation. For this, the neurons are positioned on a circle, and their relative ordering is determined by the clustering algorithm, so that two highly correlated neurons are also closely positioned on the circle. The neurons are then colored according to the average timing of their activation during the SBEs, and linked by the line colored according to the level of correlation between them. The resulting construction (henceforth termed correlation circle) lets us extract the information about the role of the network’s functional organization (the structure of correlations) in supporting certain spatio-temporal patterns of activity propagation (causal motifs). For the case of medium-sized cultured networks (shown in figure 2(d)), we observe that there are no obvious causal relations between the neurons. Different neurons in the network are activated almost simultaneously, and the level of correlations between different pairs of neurons is the same. As we show in the next section, the picture changes drastically when the activity of large cultured networks is similarly analyzed.

The generation of synchronized bursting events series, as well as some of its salient statistical properties, can be successfully captured by the dynamical-synapse-soma (DSS) model of neuronal networks, proposed by Volman *et al* [15], in which both neurons and synapses are described as dynamical elements (appendix B). Earlier, it was shown that the model recovers correctly the observed statistical scaling properties of cultured network’s spontaneous activity: it generates

synchronized bursting events separated by long (seconds to minutes) periods of sporadic activity. The internal dynamics of neurons during the SBE are also well captured by such a model neuronal network with uniform synaptic connectivity. In figure 3(d) we show the projection of the neuron correlation matrix (figure 3(c)) onto a physical space of a model network. The result is a network with uniform connectivity. The above construction may also be compared with the actual matrix of synaptic strengths projected onto a physical space of model network’s ‘electrodes’. For a pair of mutually connected neurons, however, one must consider two distinct cases, as the strength of the connection from the i th to j th neuron is not necessarily the same as the connection from the j th to i th neuron. Both of these cases are shown in figures 3(a) and (b) to demonstrate the difference.

3. Overlapping unitary networks—experimental observations

For the larger cultured networks, when the SBE correlation matrices are evaluated and re-ordered (as explained in appendix A), hidden structures are revealed. In particular, the re-ordered SBE correlation matrices were found to exhibit clear organizational motifs of blocks and strips with higher correlations, which reflect the existence of distinct sub-groups of SBEs (figures 4(a) and (b)). A block in the correlation matrix represents a sub-group of SBEs with higher

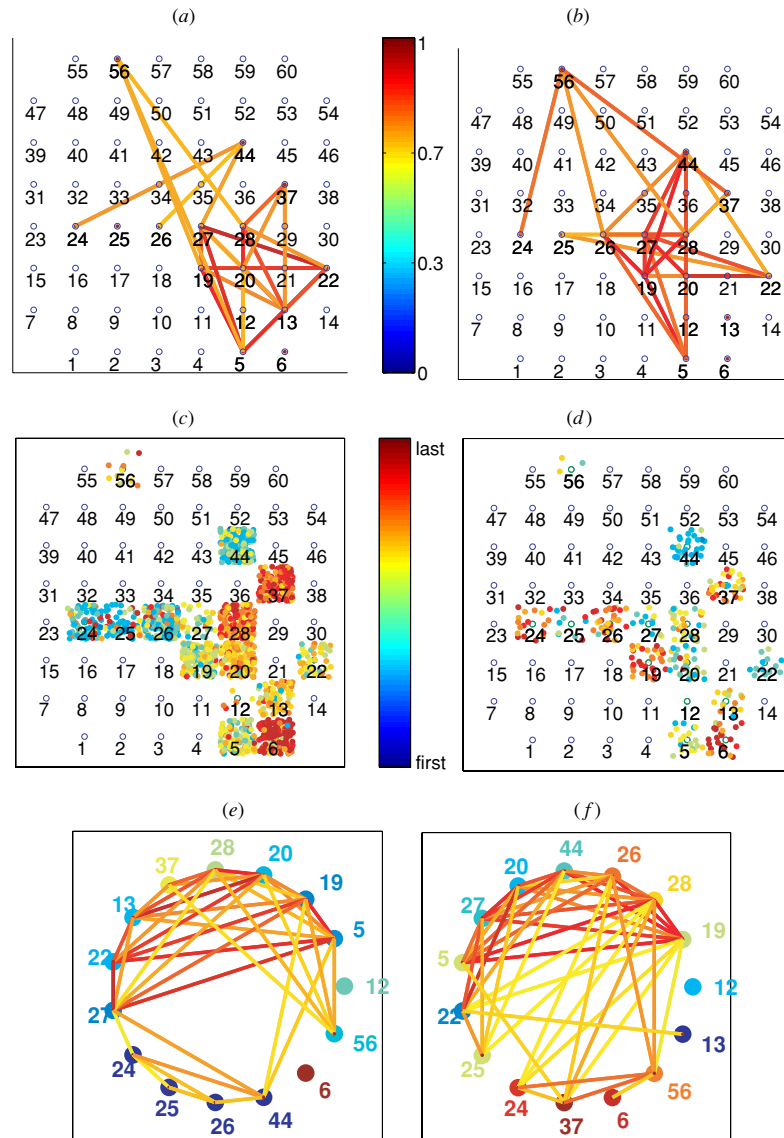


Figure 5. The internal dynamics of neurons during the SBE, for a typical large-sized cultured network which exhibits three kinds of SBEs (the corresponding SBE matrix is shown in figure 4(a)). The correlation analysis has been performed separately for the SBE series corresponding to each one of the larger blocks (bottom-left and upper-right blocks from figure 4(a)). (a), (b) Physical space projections of neuron correlation matrices for the two larger groups, shown to demonstrate the different patterns of correlations in the activity of neurons. (c), (d) The corresponding maps of activity propagation through a network. The activity propagates from the early activated neurons (blue) to the late activated ones (red). (e), (f) The corresponding correlation circles for the two groups of SBEs, shown to demonstrate the existence of context-dependent causal relations between the neurons. For example, the activation timing of neuron 24, as well as its pattern of correlations with other cells, is different for the two classes of SBEs.

inter-correlations between SBEs within the sub-group and lower correlations with the other SBEs. A strip (band) represents a sub-group of SBEs that has high correlations with all the SBEs. From a dynamical systems perspective, each sub-group of SBEs represents a chaotic attractor with its own specific internal dynamics [18].

The non-arbitrary dynamics of these large networks is revealed when looking at the temporal ordering of SBEs belonging to the different groups. Again, we use a color code to distinguish between SBEs belonging to the different sub-groups. In the middle panel of figure 4 we show an example

of such a colored sequence, constructed for the SBE series of a typical large cultured network exhibiting three kinds of bursting events (SBE correlation matrix of figure 4(a)). The different colors (green, red and blue) are associated with different sub-groups of SBEs from the corresponding SBE correlation matrix. The resulting construction clearly discloses the non-uniform temporal ordering of different synchronized bursting events.

To further test whether each group of SBEs might be related to a certain pattern of neuronal activities, in [8] the inter-neuron correlation matrices have been computed

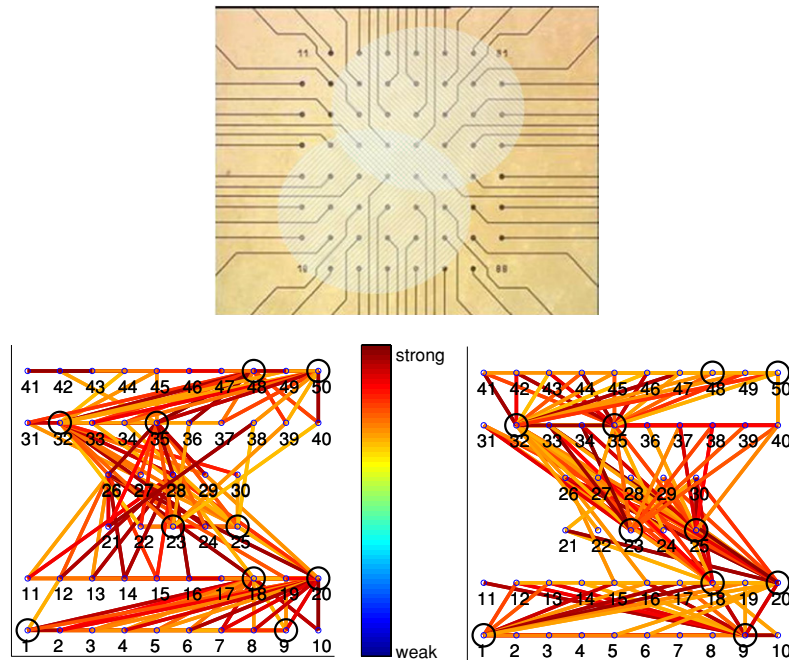


Figure 6. Top: model paradigm for the overlapping networks simulation. The model network is composed of two sub-networks, which share some neurons. The schematic representation of model networks is shown on top of the electrode array, to stress that model neurons should be viewed as representing the activity of some region in a network. Bottom: the pattern of synaptic connections is shown, to illustrate that the network’s connectivity is not uniform. The strength of synaptic connections scales according to the corresponding color code. Inhibitory neurons of the model network are marked with circles.

and analyzed (see also appendix A for technical details). The matrices, computed separately for each type of SBE, disclose the relations between different neurons during bursts of different types. For illustration, we bring, in figure 5, the projections of neuron correlation matrices onto the physical space of network’s electrodes, as obtained for two larger blocks of SBEs from figure 4(a). We observe that each sub-group of SBEs has its own characteristic correlation (activity or functional connectivity) network. In addition, the maps of activity propagation, shown in figures 5(c) and (d), indicate that the causal relations between the neurons also depend on the sub-class of SBEs under consideration. Put together, these observations suggest that large cultured networks are able to sustain different spatio-temporal patterns of neurons’ collective activity. In the next section, we investigate the possible origin of this kind of dynamics.

4. Modeling of overlapping unitary networks

The above observations of large networks’ activity indicate that the appearance of spatially and temporally structured activity might reflect the underlying networks’ synaptic connectivity. It has been proposed that the existence of sub-groups of SBEs reflects the co-existence of functionally distinguishable coupled elementary networks [8]. Therefore, the combined network can generate different kinds of SBEs, each with its own internal pattern of neuronal activity. In this picture, each kind of SBE is generated under the dominance of a different subnetwork of neuronal connectivity.

To explore the above hypothesis, we devised an extension of the DSS model, whereby we consider two overlapping neuronal networks. Specifically, each subnetwork contains 20 neurons, and both subnetworks share 10 neurons. Inside each of the subnetworks, the connectivity is all-to-all. As for the unitary model networks, we set 20% of the neurons to be inhibitory, and distribute them evenly throughout the subnetworks. The schematic representation of such networks is shown in figure 6 (top). The neuronal connectivity in this new network is clearly not uniform, as seen also from the pattern of synaptic connections in figure 6 (bottom). These overlapping networks are then allowed to evolve according to equations (B.1)–(B.3), generating synchronized bursting events, as explained earlier.

A brief glance at the SBEs’ correlation matrix (figure 7(a)) discloses the existence of SBEs with different internal structure. Indeed, for the different model networks with pre-imposed structured connectivity of synaptic contacts, we found that the corresponding SBE matrices exhibit block-partitioning. Some additional examples are shown in figures 7(b)–(d). We explain these results as follows: in principle, every neuron in the network has equal probability of triggering a synchronized burst. Yet, the pre-imposed connections architecture allows the collective activity to propagate only along certain routes. In the case of two overlapping networks considered here, there are two modes of activity propagation. In each mode, the activity starts in one of the subnetworks and then gradually spreads, through the shared region, to the second subnetwork. Besides these two basic modes of propagation, it is also possible to observe

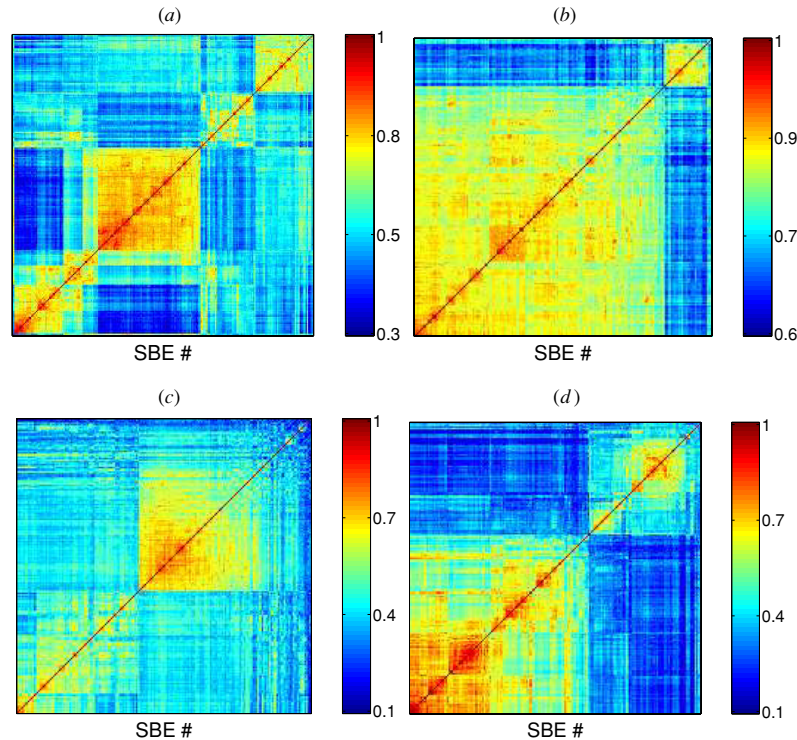


Figure 7. Examples of SBE correlation matrices obtained for different model networks. The level of correlations for each matrix scales according to the corresponding color codes. (a) The SBE correlation matrix obtained for the model of two overlapping networks. In this case, the matrix exhibits block-partitioning, with each block corresponding to the scenario in which one of the sub-networks is dominant. (b) The SBE correlation matrix obtained for the model network in which the distribution of neuronal connectivity is bi-modal. (c) The SBE correlation matrix obtained for the overlapping networks' model, in which the average synaptic strength between the neurons in one of the sub-networks is higher than the average synaptic strength in the second sub-network. (d) The SBE correlation matrix obtained for the model network, which is composed of two sub-networks having several axons linking them. This case may be looked upon as a 'weak connection limit' of the overlapping networks' model.

higher-order events, when the activity may bounce back and forth between the two subnetworks for a certain time. These higher-order events lead to the appearance of additional smaller blocks in SBE matrix (the two upper blocks in the matrix shown in figure 7(a)).

To ensure that the results shown in figure 7 are not an outcome of random effects, but correspond to the structural organization of network's elements, we have performed two tests. First, we calculated the SBE correlation matrices for model networks with uniform connectivity. This computation yielded a correlation matrix in which all of the bursting events had the same level of correlation between them. As a second test, we created random surrogate matrices (with the same mean level of correlations as for the matrices shown in figure 7) and applied the clustering algorithm to these matrices. The resulting re-ordered random matrices did not exhibit any block-partitioning structure. Hence, the structured activity of our model network is determined by the structural organization of network's elements.

To further verify the hypothesis about the correspondence between the imposed form and the resulting spatio-temporal patterns of activity, we performed the correlation analysis on the model network's SBEs corresponding to each of the two dominant blocks in figure 7(a). As shown in figure 8, the resulting neuron correlation matrices, when projected onto

the network's 'real space' representation, reveal interesting features. For example, we observe that in some cases the activity of a pair of neurons that have no physical contact is, nevertheless, correlated (a line in the correlations connectivity network). On the other hand, some physically connected pairs show no contact at all in the correlations connectivity networks.

Additional information about the effects of imposing structural constraints on networks' activity is obtained from analysis of corresponding correlation circles. As illustrated in figures 8(e) and (f), for the overlapping networks case, the positioning of inhibitory neurons on the correlation circle depends on the type of the SBE under consideration. Hence, when a network's architecture is non-uniform, the behavior of inhibitory neurons is context-dependent, i.e. it depends on the overall activity of other neurons in the network.

5. The effect of a regulating current

The model network presented so far is able to account for the emergence of SBEs with different spatio-temporal structures. This has been achieved by dividing the network into two smaller coupled subnetworks. Different SBEs originated because at different times different subnetworks were dominant.

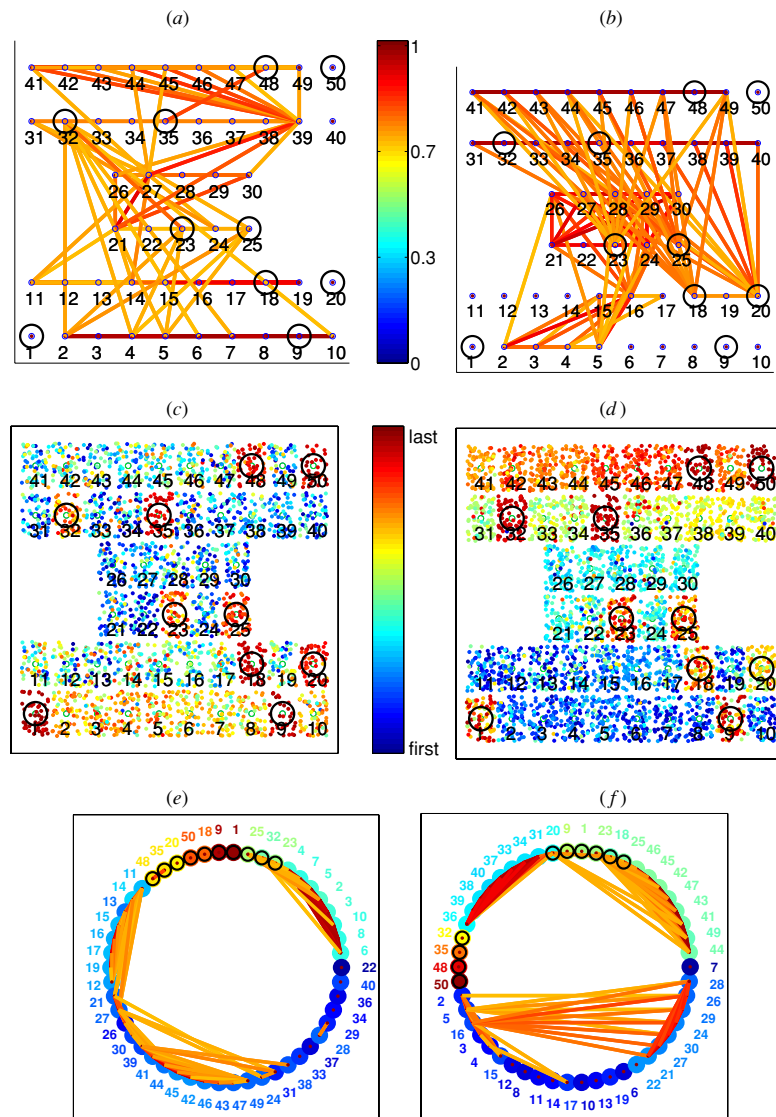


Figure 8. The internal neuron dynamics for a model of two overlapping unitary networks (the corresponding SBE matrix is shown in figure 7(a)). The correlation analysis has been performed separately for the SBEs corresponding to each of the larger blocks (bottom-left and middle blocks from figure 7(a)). (a), (b) Physical space projections of neuron correlation matrices for the two larger groups, shown to demonstrate the different patterns of correlations in the activity of neurons. For example, the correlation between neurons nos. 20, 40 depends on the class of the SBE under consideration. (c), (d) The corresponding maps of activity propagation through a network. The activity propagates from the early activated neurons (blue) to the late ones (red). (e), (f) The corresponding correlation circles for the two groups of SBEs are shown to demonstrate the existence of context-dependent causal relations between the neurons. For example, the relative correlations of inhibitory neurons (marked with circles), as well as the timing of their activation, depend on the type of the SBE under consideration. In light of these results, we note that the observations shown in figure 5 might represent the recording from several overlapping networks. For example, sampling and analyzing neurons nos. 30–50 yields results similar to those shown in figure 5.

The additional feature in the activity of large cultured neuronal networks is a unique temporal ordering of different SBEs. Such ability to regulate the relative temporal ordering of different SBEs might endow the networks with higher plasticity and complexity [10]. In principle, the temporal ordering of different model SBEs might be controlled by imposing activity-dependent dynamics on the additional background current I_{ad} provided there exists a biological correlate for this current. Such a correlate might be readily provided by glia cells surrounding the neurons. Indeed, there is evidence that neurons and glia maintain intricate dialogue,

exchanging information on the molecular level [19–21]. To provide an instructive example, it has recently been shown that astrocytes synchronize neuronal activity by generating glutamate-related currents. These currents, shown in figure 9(a), are non-synaptic, as their decay time (~ 700 ms) is much larger than that of the synaptic ones.

To verify the assumption of possible regulatory role for the background currents, we sequentially elevate I_{ad} in structurally different parts of a network using the following procedure: first, for a period of 20 min one of the larger subnetworks is subjected to higher average levels of the background current

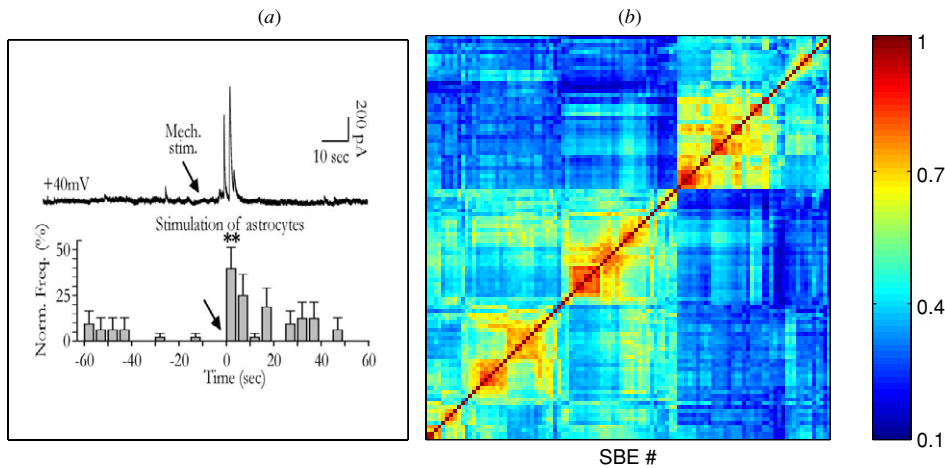


Figure 9. (a) Stimulation of astrocytes generates slow transient currents (STC) in pyramidal neurons. The top trace illustrates slow transient currents induced by the glutamate released from astrocytes. The histogram (bottom trace) is shown to demonstrate the increase in STC frequency, following the stimulation of astrocytes. Reproduced, with permission, from [22], © (2004) by the Society for Neuroscience. (b) By controlling the dynamics of the additional current I_{ad} it is possible to modulate the expression of networks' spatio-temporal patterns. When the spatio-temporal profile of I_{ad} has been modulated, the temporal ordering of different SBEs changed accordingly, as explained in the text. The SBEs of the first block (event nos. 1–65) correspond to the domination of one of the larger sub-networks, while events 66–105 (second block) to the prevalence of the second larger subnetwork.

(while in other parts of a network I_{ad} is suppressed). Then, the same procedure is performed for the second subnetwork for another 20 min. The resulting SBE correlation matrix is shown in figure 9(b). All of the events have been classified as belonging to one of the two groups, corresponding to two distinct 'stimulation protocols'. We conclude that, by controlling the spatio-temporal dynamics of the additional background current I_{ad} , it might be possible to regulate the temporal ordering of different SBEs.

6. Conclusion and outlook

In this work, we have investigated the possible causes underlying the appearance of structured spatio-temporal patterns in the activity of neuronal networks. We have shown that, when a network is endowed with structured synaptic connectivity, it is possible to obtain structured activity, manifested in the block partitioning of SBE correlation matrix. In this case, the spatio-temporal correlations between different neurons also acquire non-trivial features. In addition, we have shown how, within a given network's architecture, it is possible to selectively regulate the appearance of different patterns by controlling the additional regulating current, I_{ad} .

From the perspective of pattern formation, or dynamical self-organization, the possibility of regulating a network's structured activity suggests that the observed complex neuronal dynamics might be supported by some underlying feedback mechanism with regulatory features. An instructive analogy borrowed from physics would be the complex spatio-temporal behavior formed on top of the more regular, underlying dynamical behavior in fluid flow systems [23]. In this regard, it is interesting to ask whether the recorded neuronal activity represents only a part of the underlying dynamics.

Partial answers to these questions may be provided from the vast amount of recent experimental evidence regarding the complex spatio-temporal chemical activity in the glia web and the interaction between neurons and glia cells [20–22]. Intra-cellular regulatory mechanisms enable even individual glia cells to function as excitable elements capable of using energy to generate internal structured calcium dynamics. Such noise-induced dynamics can be generated, for example, by an internal coherence (synchronized coupling) resonance mechanism [24]. As another example, astro-glia cells surrounding synaptic terminals could temporarily shunt or enhance synaptic transmission by dynamically modulating the concentration of glutamate neuro-transmitter [21]. It seems possible that the special excitable media capabilities of the glia fabrics of generating chemical waves, together with their special interaction with the neuronal and synaptic activity, could provide the required mechanisms.

These considerations lead us to speculate that real neuronal networks might utilize mechanisms other than those of synaptic transmission in order to regulate the expression of different spatio-temporal activity patterns. The repertoire of possible activity states is determined by the underlying architecture of the network. Actually expressed patterns, however, are selected from this repertoire by means of complex regulatory pathways (such as chemical wave signaling or glia regulation of synaptic strength) [25, 26]. Put together, these intricate regulatory mechanisms utilized by neuronal networks might provide some answers about how the brain stores and transmits information.

Acknowledgments

The authors would like to thank Peter Jung, Herbert Levine and Eugene Izhikevich for stimulating conversations and valuable

comments on an earlier version of the manuscript. We are most grateful to Maria Cecilia Angulo for permission to present her measurements in figure 9(a). This research has been supported in part by the Maguy-Glass chair in Physics of Complex Systems, the ISF and the Adams super-center for brain studies.

Appendix A. Analysis methods

Due to the long-term recordings, the activity of a typical cultured network should be analyzed on different levels, ranging from the investigation of the statistical characteristics of networks' activity over long times (hours), to the analysis of the activity on millisecond level (the dynamics of neurons during the bursting event).

To explore the long-term activity of a network, the recorded activity is converted into a binary sequence: the time axis is partitioned according to the temporal width of a typical SBE, and the '1's of the sequence mark the locations of events. The resulting binary vector then corresponds to the series of bursting events. The statistical characteristics of the SBE time series are then accessed by analyzing the rate of bursting events' generation and the distributions of inter-burst-interval series [11, 15].

At the other side of the temporal spectrum, a high temporal resolution of recordings allows one to investigate the dynamics of neurons during the synchronized bursting event. To check whether the SBEs can be sorted into distinct sub-groups with similar internal patterns of neuronal activity, the inter-SBE correlation matrix (or event correlations), $EC_{n,m}$ [8], is computed:

$$EC_{n,m} = \text{Max} \left\{ \sum_{i=1}^N C_{n,m}^i(t) \right\}. \quad (\text{A.1})$$

In the above definition, $C_{n,m}^i(t)$ denotes the cross-correlation between the activity of the i th neuron in the n th and m th SBEs, and the maximum is taken over the time window corresponding to the duration of a typical bursting event. Next, the correlation matrix is clusterized using the standard dendrogram clustering method [27]. The resulting reordered correlation matrices of some networks exhibit clear organizational motifs of blocks and strips with higher correlations which reflect the existence of distinct sub-groups of SBEs.

To study temporal relations between different neurons we calculate, for each sub-group of SBEs, its corresponding neuron correlation matrix. The correlation coefficient between the activity of a pair of neurons is computed as follows,

$$C_{ij} = \frac{\langle (X_i(t) - \mu_i)(X_j(t) - \mu_j) \rangle}{\sigma_i \sigma_j} \quad (\text{A.2})$$

where X_i and X_j are the activities of neurons i and j , with the corresponding means μ_i and μ_j and sample standard deviations σ_i and σ_j . The averaging is performed over the sub-group of SBEs. The correlation coefficients for all pairs of neurons are computed, yielding the correlation matrix C_{ij} .

Further, to study the propagation of activity during the burst, a temporal location of each neuron in the burst is

evaluated. The temporal location, T_n^i , of the i th neuron during the n th SBE is defined as

$$T_n^i = \frac{\int (t - T_n) D_n^i(t - T_n) dt}{\int D_n^i(t - T_n) dt} \quad (\text{A.3})$$

where T_n is the 'temporal location' of the n th SBE which is the combined 'center of mass' of all the neurons, and $D_n^i(t)$ is the activity rate of the i th neuron [8]. This analysis discloses that each type of SBEs has its own characteristic spatio-temporal pattern of activity propagation.

Using the above definitions, it is possible to determine whether the pattern of correlations in the correlation matrix can also be related to the characteristic pattern of spatio-temporal propagation (temporal ordering of neurons during the burst). This goal is achieved in two steps. First, the neuron correlation matrix is represented as a connectivity network in the cultured network physical space. The idea is similar to the way the coherence matrices of recorded brain activity are mapped onto connectivity networks according to the electrode locations in the cortex. In the case of cultured network, the color lines are simply drawn between the locations of each two recording electrodes to represent the level of neuron correlations C_{ij} .

An additional information about causal relations between neurons (the timing of activity propagation) versus the functional organization of a network, is obtained by constructing the correlation circles. In this representation, the neurons are positioned on the circle, with their relative ordering determined by the clustering algorithm, so that a pair of highly correlated neurons are also closely positioned on the circle. Pairs of neurons are then linked by lines colored according to the value of C_{ij} between them. To capture the causal relations between the neurons, the vertices (which represent the active electrodes of the network) are colored according to the average timing of their activation, i.e. the average of T_n^i for events belonging to the same sub-group of SBEs.

Appendix B. The dynamical soma and synapse model

Computer modeling can serve as an equally powerful research tool in the studies of biotic systems [28, 29], provided it is utilized and analyzed in a proper manner adapted to the special autonomous (regulating) nature of these systems. Guided by the above realization, we have developed a new model in which both the neurons and the synapses connecting them are described as dynamical elements [15]. To model the neurons, we have adopted the Morris–Lecar [30] (M-L) dynamical description. The Morris–Lecar model reads

$$\dot{V} = -I_{\text{ion}}(V, W) + I_{\text{ext}}(t) \quad (\text{B.1})$$

$$\dot{W} = \phi \frac{W_{\infty}(V) - W}{\tau_W} \quad (\text{B.2})$$

with $I_{\text{ion}}(V, W)$ representing the contribution of the internal ionic Ca^{2+} , K^+ and leakage currents, with their corresponding channel conductivities g_{Ca} , g_{K} and g_{L} being constant

$$I_{\text{ion}}(V, W) = g_{\text{Ca}} m_{\infty}(V)(V - V_{\text{Ca}}) + g_{\text{K}} W(V - V_{\text{K}}) + g_{\text{L}}(V - V_{\text{L}}). \quad (\text{B.3})$$

The additional current I_{ext} appearing in equation (B.1) represents all the external current sources stimulating the neuron, such as signals received through its synapses, gliaderived currents, artificial stimulations as well as any noise sources. In the absence of any such stimulation, the fraction of open potassium channels, W , relaxes towards its limiting curve $W_{\infty}(V) = \frac{1}{2}(1 + \tanh(\frac{V-V_1}{2V_2}))$, within a characteristic time scale given by

$$\tau_W(V) = \frac{1}{\cosh(\frac{V-V_1}{2V_2})}. \quad (\text{B.4})$$

The limiting dynamics of calcium channels are described by another sigmoid function:

$$m_{\infty}(V) = \frac{1}{2} \left(1 + \tanh \left(\frac{V - V_3}{V_4} \right) \right). \quad (\text{B.5})$$

In our numerical simulations, we have used the following values: $g_{\text{Ca}} = 1.1 \text{ mS cm}^{-2}$, $g_{\text{K}} = 2.0 \text{ mS cm}^{-2}$, $g_{\text{L}} = 0.5 \text{ mS cm}^{-2}$, $V_{\text{Ca}} = 100 \text{ mV}$, $V_{\text{K}} = -70 \text{ mV}$, $V_{\text{L}} = -35 \text{ mV}$, $V_1 = 10 \text{ mV}$, $V_2 = 14.5 \text{ mV}$, $V_3 = -1 \text{ mV}$, $V_4 = 15 \text{ mV}$, $\phi = 0.3$. With such a choice of parameters, the critical current I_c , separating the quiescent and spiking phases, is set $I_c = 0$.

According to the theory of neuronal group selection, the size of the brain's basic functional assembly varies between 50 and 10^4 cells. Motivated by this, and by the notion of unitary networks (as explained in the main text), we study the dynamics of networks composed of 20 – 60 cells. To follow physiological data [31], 20% of the cells are usually set to be inhibitory.

The neurons in the model network exchange action potentials via the multi-state dynamic synapses, as described by Tsodyks *et al* [17]. In this model, the effective synaptic strength evolves according to the following equations:

$$\dot{x} = \frac{z}{\tau_{\text{rec}}} - ux\delta(t - t_{\text{sp}}) \quad (\text{B.6})$$

$$\dot{y} = -\frac{y}{\tau_{\text{in}}} + ux\delta(t - t_{\text{sp}}) \quad (\text{B.7})$$

$$\dot{z} = \frac{y}{\tau_{\text{in}}} - \frac{z}{\tau_{\text{rec}}}. \quad (\text{B.8})$$

Here, x , y and z are the fractions of synaptic resources in the recovered, active and inactive states, respectively. The time series t_{sp} denote the arrival times of pre-synaptic spikes, τ_{in} is the characteristic time of post-synaptic currents (PSCs) decay and τ_{rec} is the recovery time from synaptic depression.

The variable u describes the effective use of synaptic resources by the incoming spike. For facilitating synapses, it obeys the following dynamic equation:

$$\dot{u} = -\frac{u}{\tau_{\text{facil}}} + U_0(1 - u)\delta(t - t_{\text{sp}}) \quad (\text{B.9})$$

where the parameter U_0 determines the increase in the value of u with each spike. If no spikes arrive, the facilitation parameter decays to its baseline value with the time constant τ_{facil} . For the depressing synapses (as is the case when post-synaptic neuron is excitatory) one has $\tau_{\text{facil}} \rightarrow 0$, and $u \rightarrow U_0$ for each spike.

The effective synaptic current of a neuron i is obtained by summing all of its j synaptic currents:

$$I_{\text{syn}}^i = \sum_{j \neq i} A_{ij} y_j(t) \quad (\text{B.10})$$

where the parameter A_j is the maximal value of synaptic strength.

The values of parameters control the ability of the system to exhibit modes of correlated activity. In our studies (unless indicated otherwise), we assign to the network the parameters specified below, using the following notations: I indicates inhibitory neurons and E the excitatory ones. For example, $\tau_{\text{rec}}(E \rightarrow I)$ refers to the recovery time of a synapse transmitting input to an inhibitory neuron from excitatory one. Hence, we set $\tau_{\text{rec}}(I \rightarrow I) = 200 \text{ ms}$, $\tau_{\text{rec}}(E \rightarrow I) = 200 \text{ ms}$, $\tau_{\text{rec}}(I \rightarrow E) = 1200 \text{ ms}$, $\tau_{\text{rec}}(E \rightarrow E) = 1200 \text{ ms}$, $U_0(I \rightarrow I) = 0.5$, $U_0(E \rightarrow I) = 0.5$, $U_0(I \rightarrow E) = 0.08$, $U_0(E \rightarrow E) = 0.08$, $A(I \rightarrow I) = 9$, $A(E \rightarrow I) = 9$, $A(E \rightarrow E) = 2.2$, $A(I \rightarrow E) = 6.6$. Actual values for each neuron were then generated as reported in [17]. We set $\tau_{\text{in}} = 6 \text{ ms}$ for all neurons. In addition, due to the small size of our simulated network, we chose $\tau_{\text{facil}} = 2000 \text{ ms}$ for all inhibitory neurons.

To complete the picture, we need to provide a mechanism responsible for the generation of spontaneous activity in the isolated network. To simulate this, each neuron is subject to the fluctuating additional current

$$I_{\text{ad}}(t + 1) = I_{\text{ad}}(t) + \xi; \quad \xi = \begin{cases} +\epsilon, & p = 0.5 \\ -\epsilon, & p = 0.5 \end{cases}. \quad (\text{B.11})$$

The fluctuating current may drive the neuron beyond the firing threshold, thus enabling it to generate spike and trigger the SBE. To keep a proper balance between the above current and inputs received from other neurons via the synaptic connections, the additional current I_{ad} is limited to the range $I_{\text{low}} \leq I_{\text{ad}} \leq I_{\text{high}}$. The total current seen by a neuron at any time is a sum of $I_{\text{syn}}(t)$ and $I_{\text{ad}}(t)$.

References

- [1] Maas W and Bishop C B (ed) 1999 *Pulsed Neural Networks* (Cambridge, MA: MIT Press)
- [2] Dayan P and Abbott L F 2001 *Theoretical Neuroscience* (Boston, MA: MIT Press)
- [3] Kandel E R, Schwartz J H and Jessell T M 2000 *Principles of Neural Science* (New York: McGraw-Hill)
- [4] Hilgetag C C, Burns G A, O'Neill M A, Scanell J W and Young M P 2000 Anatomical connectivity defines the organization of clusters of cortical areas in macaque monkey and cat *Phil. Trans. R. Soc. B* **355** 91–110
- [5] Towle V L, Carder R K, Khorasani L and Lindberg D 1999 Electrographic coherence patterns *J. Clin. Neurophysiol.* **16** 528–47
- [6] Stephan K E, Burns G A, O'Neill M A, Young M P and Kotter R 2000 Computational analysis of functional connectivity between areas of primate cerebral cortex *Phil. Trans. R. Soc. B* **355** 111–26
- [7] Segev R, Benveniste M, Shapira Y and Ben-Jacob E 2003 Formation of electrically active clusterized neural networks *Phys. Rev. Lett.* **90** 168101
- [8] Segev R, Baruchi I, Hulata E and Ben-Jacob E 2004 Hidden neuronal correlations in cultured networks *Phys. Rev. Lett.* **92** 118102
- [9] Baruchi I and Ben-Jacob E 2004 Functional holography of recorded neuronal networks activity *Neuroinformatics* **2** 333–51
- [10] Hulata E, Baruchi I, Segev R, Shapira Y and Ben-Jacob E 2004 Self-regulated complexity in cultured neuronal networks *Phys. Rev. Lett.* **92** 198105

- [11] Segev R, Benveniste M, Hulata E, Cohen N, Paleski A, Kapon E, Shapira Y and Ben-Jacob E 2002 Long term behavior of lithographically prepared in-vitro neural networks *Phys. Rev. Lett.* **88** 118102
- [12] Ayali A *et al* 2004 Contextual regularity and complexity of neuronal activity: from stand-alone cultures to task-performing animals *Complexity* **9** 25–32
- [13] Baruchi I 2003 Formation of hidden spatio-temporal correlations observed in the lithographically prepared neuronal networks *MSc Thesis* Tel-Aviv University
- [14] Gabay T, Jacobs E, Ben-Jacob E and Hanein Y 2005 Engineered self-organization of neural networks using carbon nanotubes clusters *Physica A* **350** 611–21
- [15] Volman V, Baruchi I, Persi E and Ben-Jacob E 2004 Generative modeling of regulated dynamical behavior in cultured neuronal networks *Physica A* **335** 249–78
- [16] Persi E, Horn D, Volman V and Ben-Jacob E 2004 Modelling of synchronized bursting events: the importance of inhomogeneity *Neural Comput.* **16** 2577–95
- [17] Tsodyks M, Uziel A and Markram H 2000 Synchrony generation in recurrent networks with frequency-dependent synapses *J. Neurosci.* **20** RC50
- [18] Volman V, Baruchi I and Ben-Jacob E 2004 Self-regulated homoclinic chaos in cultured neuronal networks *Proc. 8th Experimental Chaos Conference*
- [19] Nadkarni S and Jung P 2004 Spontaneous oscillations of dressed neurons: a new mechanism for epilepsy? *Phys. Rev. Lett.* **91** 268101
- [20] Laming P R, Kimelberg H, Robinson S, Salm A, Hawrylak N, Muller C, Roots B and Ng K 2000 Neuronal-glia interactions and behavior *Neurosci. Behav. Rev.* **24** 295–340
- [21] Araque A, Parpura V, Sanzgiri R P and Haydon P G 1999 Tripartite synapses: glia, the unacknowledged partner *Trends Neurosci.* **22** 208–15
- [22] Angulo M C, Kozlov A S, Charpak S and Audinat E 2004 Glutamate released from glial cells synchronizes neuronal activity in the hippocampus *J. Neurosci.* **24** 6920–7
- [23] Daniels K E and Bodenschatz E 2002 Defects turbulence in inclined layers correction *Phys. Rev. Lett.* **88** 034501
- [24] Shuai J W and Jung P 2003 Selection of intracellular calcium patterns in a model with clustered ca release channels *Phys. Rev. E* **67** 031905
- [25] Edelman G M and Mountcastle V B 1979 *The Mindful Brain: Cortical Organization and the Group-Selective Theory of Higher Brain Function* (Boston, MA: MIT Press)
- [26] Izhikevich E M, Gally J A and Edelman G M 2004 Spike-timing dynamics of neuronal groups *Cereb. Cortex* **14** 933–44
- [27] Press W H, Teukolsky S A, Vetterling W T and Flannery B P 1992 *Numerical Recipes in C* (Cambridge: Cambridge University Press)
- [28] Ben-Jacob E, Cohen I and Levine H 2001 Cooperative self-organization of microorganisms *Adv. Phys.* **49** 395–554
- [29] Levine H and Ben-Jacob E 2004 Physical schemata underlying biological pattern formation—examples, issues and strategies *Phys. Biol.* **1** 14–22
- [30] Morris C and Lecar H 1981 Voltage oscillations in the barnacle giant muscle fiber *Biophys. J.* **35** 193–213
- [31] Abeles M 1991 *Corticonics* (Cambridge: Cambridge University Press)